STEM CELLS

CANCER STEM CELLS

# Bone Environment is Essential for Osteosarcoma Development from Transformed Mesenchymal Stem Cells

RUTH RUBIO,[a] ANDER ABARRATEGI,[b] JAVIER GARCIA–CASTRO,[b] LUCIA MARTINEZ–CRUZADO,[c] CARLOS SUAREZ,[c] JUAN TORNIN,[c] LAURA SANTOS,[c] AURORA ASTUDILLO,[c] ISABEL COLMENERO,[d] FRANCISCA MULERO,[e] MICHAEL ROSU–MYLES,[f] PABLO MENENDEZ,[a,g,h] RENE RODRIGUEZ[a,c]

**Key Words.** Mesenchymal stem cells • Osteosarcoma • Bone • Tumoral microenvironment • p53 • Rb • Bone morphogenetic protein-2 • WNT signaling

[a]GENyO, Centre for Genomics and Oncological Research, Pfizer/University of Granada/Andalusian Government, Granada, Spain; [b]Unidad de Biotecnología Celular, Área Biología Celular y del Desarrollo, Instituto de Salud Carlos III, Majadahonda, Madrid, Spain; [c]Hospital Universitario Central de Asturias and Instituto Universitario de Oncología del Principado de Asturias, Oviedo, Spain; [d]Servicio de Anatomía Patológica, Hospital Universitario Niño Jesús, Madrid, Spain; [e]Spanish National Cancer Research Center (CNIO), Molecular Imaging Core Unit, Madrid, Spain; [f]Health Canada Centre for Biologics Research, Biologics and Genetic Therapies Directorate, Health Canada, Ottawa, Ontario, Canada; [g]Instituciò Catalana de Reserca i Estudis Avançacts (ICREA), Barcelona, Spain; [h]Josep Carreras Leukemia Research Institute and Cell Therapy Program, Facultat de Medicina, Barcelona University, Barcelona, Spain

Correspondence: Rene Rodriguez Ph.D., Hospital Universitario Central de Asturias and Instituto Universitario de Oncología del Principado de Asturias, Laboratorio 2 ORL–IUOPA, 33006 Oviedo, Spain. Telephone: +34-985-108000, ext. 38524; Fax: +34-985-108015; e-mail: renerg@ficyt.es; or Pablo Menendez, Ph.D., Josep Carreras Leukemia Research Institute, Facultat de Medicina, University of Barcelona, Carrer de Casanova, 143, 08036 Barcelona, Spain. Telephone: +34-935572810; Fax: +34-933231751; e-mail: pmenendez@carrerasresearch.org

Received July 3, 2013; accepted for publication January 2, 2014; first published online in STEM CELLS EXPRESS January 20, 2014.



http://dx.doi.org/10.1002/stem.1647

## ABSTRACT

**The cellular microenvironment plays a relevant role in cancer development. We have reported that mesenchymal stromal/stem cells (MSCs) deficient for p53 alone or together with RB ($p53^{-/-}RB^{-/-}$) originate leiomyosarcoma after subcutaneous (s.c.) inoculation. Here, we show that intrabone or periosteal inoculation of $p53^{-/-}$ or $p53^{-/-}RB^{-/-}$ bone marrow- or adipose tissue-derived MSCs originated metastatic osteoblastic osteosarcoma (OS). To assess the contribution of bone environment factors to OS development, we analyzed the effect of the osteoinductive factor bone morphogenetic protein-2 (BMP-2) and calcified substrates on $p53^{-/-}RB^{-/-}$ MSCs. We show that BMP-2 upregulates the expression of osteogenic markers in a WNT signaling-dependent manner. In addition, the s.c. coinfusion of $p53^{-/-}RB^{-/-}$ MSCs together with BMP-2 resulted in appearance of tumoral osteoid areas. Likewise, when $p53^{-/-}RB^{-/-}$ MSCs were inoculated embedded in a calcified ceramic scaffold composed of hydroxyapatite and tricalciumphosphate (HA/TCP), tumoral bone formation was observed in the surroundings of the HA/TCP scaffold. Moreover, the addition of BMP-2 to the ceramic/MSC implants further increased the tumoral osteoid matrix. Together, these data indicate that bone microenvironment signals are essential to drive OS development.** STEM CELLS *2014;32:1136–1148*

## INTRODUCTION

Over the last years, mesenchymal stromal/stem cells (MSCs) and/or MSC-derived lineage-specific progenitors have been proposed as the cell of origin for certain soft tissue sarcomas (STS) and primary bone sarcomas [1–4]. Within bone sarcomas, osteosarcoma (OS) constitutes the most frequent one comprising approximately 20% of new diagnosis [5, 6]. The prevalence of OS correlates with skeletal growth presenting the main incidence peak in the second decade of life. OS is also relatively common in elderly adults and is often preceded by certain genetic predispositions such as the Li-Fraumeni syndrome or hereditary retinoblastoma [7–9]. These syndromes are caused by germline mutations of P53 and RB, respectively, and importantly, mutations in p53 and/or RB pathways are also common in sporadic OS, suggesting a relevant role for the alterations in these tumor suppressor genes in the OS development [7, 10, 11]. P53 and RB play a key role in the regulation of MSC differentiation pathways. Thus, p53 activation suppresses osteoblast differentiation by inhibiting the expression of Runx2 [12]. Conversely, p53 deletion accelerates osteoblastic differentiation while impairing osteocyte terminal maturation [13]. P53 also inhibits the adipogenic and smooth muscle differentiation programs by downregulating PPAR$\gamma$ and MYOCD, respectively [14]. On the other hand, RB was reported to regulate mesenchymal differentiation along different mesenchymal lineages, including osteoblastic, adipogenic, and myogenic through the transcriptional regulation of several lineage-specific transcription factors [15–18].

The development of p53- and/or RB-deficient mesenchymal lineage-specific mouse models supported the link between these tumor suppressors and OS [9]. Thus, the inactivation of p53 alone or in combination with RB in the osteoblastic lineage led to OS development in nearly 100% of mice [19, 20]. Similarly, the inactivation of RB and/or p53 in early mesenchymal progenitors of embryonic limb buds resulted in sarcoma development presenting a lower incidence of OS (60% in $p53^{-/-}$ mice and 20%–30% in $p53^{-/-}RB^{-/-}$ mice) and an increased incidence of poorly differentiated STS [15, 21]. Additionally, we have studied the role of p53 and/or RB deficiency in sarcomagenesis using ex vivo cultures of MSCs and have reported that $p53^{-/-}$ and $p53^{-/-}RB^{-/-}$ adipose derived-MSCs (ASCs) or bone marrow derived-MSCs (BM-MSCs) give rise to leiomyosarcoma-like tumors when injected s.c. in immunodeficient mice [22, 23]. Nevertheless, when BM-MSCs were differentiated along the osteoblastic lineage before Cre-mediated deletion of p53 and RB, they generated OS-like tumors upon s.c injection in immunodeficient mice, evidencing that the stage of differentiation seems to contribute to the sarcoma phenotype [23]. However, the possibility that undifferentiated MSCs might also represent the cell of origin for OS under the influence of certain bone microenvironment signals cannot be ruled out.

Bone morphogenetic proteins (BMPs) are instrumental in the regulation of osteogenic differentiation of MSCs during development [24]. BMP signaling transduction through Mothers Against Decapentaplegic homologs (SMAD)-dependent and SMAD-independent pathways converges at the RUNX2 gene to control osteogenic differentiation [24]. Within BMPs, BMP-2 is an osteoinductive morphogen abundant in the bone extracellular matrix with proven activity on MSCs and defined roles in bone formation processes [24, 25]. BMP-2 is extensively expressed in the growth plate, and its inhibition prevents osteogenic differentiation [26, 27]. Likewise, the loss of BMP-2 in limb bud mesenchymal tissues leads to the inability to repair postnatal fractures [28], and the co-inactivation of both BMP-2 and BMP-4 results in severe osteogenesis impairment [29]. Conversely, a short-term expression of the BMP-2 is necessary and sufficient to induce bone formation [30]. These results evidence the central role that BMP-2 plays in postnatal bone growth and bone fracture healing and support its clinical use to stimulate new bone formation [31, 32].

Besides osteogenic morphogens such as BMP-2, calcified extracellular matrix is another singular environmental factor that plays a role in bone tissues. Endosteal microenvironment is a well-defined MSC niche where cells adhere to calcified substrates and are highly exposed to calcium ions. This is the rationale for many bone regeneration strategies using calcium phosphate biomaterials, such as bioactive hydroxyapatite and tricalciumphosphate (HA/TCP) ceramic powders, as scaffolds to support the growth of MSCs in the repair of damaged bone tissue [33–35]. Likewise, OS cell lines grown onto ceramic materials showed an osteoblastic phenotype and a modified cytokine expression pattern as compared to plastic-adhered cultures [36].

Here, we wanted to assess whether the bone microenvironment is capable of redirecting the sarcomagenesis potential/phenotype of undifferentiated $p53^{-/-}$ and/or $p53^{-/-}RB^{-/-}$ MSCs. Our data show that p53 or p53/RB deficiency in undifferentiated BM-MSCs/ASCs promotes metastatic osteoblastic OS development upon intrabone or periosteal orthotopic transplantation while leiomysarcoma-like tumors are developed after s.c. inoculation of these cells [22, 23]. Furthermore, s.c inoculation of $p53^{-/-}RB^{-/-}$ BM-MSCs/ASCs together with BMP-2 or embedded into ceramic implants containing HA/TCP resulted in an increased appearance of osteogenic differentiated areas within the tumor. Overall, these data indicate that bone microenvironment signals are essential to drive in vivo the osteogenic differentiation of transformed p53- or p53/RB-deficient BM-MSCs/ASCs, eventually promoting OS development.

## Materials and Methods

### Generation of Mutant MSCs and Cell Culture

Wild type (Wt), $p53^{-/-}$, $RB^{-/-}$ and $p53^{-/-}RB^{-/-}$ BM-MSCs, and ASCs were obtained and cultured as previously described from Friend Virus B (FVB) background mice bearing alleles for either p53, RB, or both genes flanked by loxP sites [22, 23]. Mutant MSCs were generated by excision of the LoxP-flanked sequences by infection with adenoviral vectors expressing the Cre-recombinase. Successful gene knockdown was confirmed by genomic polymerase chain reaction (PCR). MSCs were tagged with green fluorescent protein (GFP) as reporter gene using the pWPI lentiviral vector (Addgene, 12254, Cambridge, MA, https://www.addgene.org/). The production of the viral particles, and the transduction of MSC cultures was performed as previously described [37]. Only early-passage (p5 to p15) MSCs were used in downstream experiments. Saos-2 cells were obtained from de ATCC and cultured as previously described [38]. Saos-2 conditioned medium was collected after 4 days of confluent culture and was concentrated using Amicon Ultra Centrifugal filters (Millipore, Billerica, MA, http://www.millipore.com) before being added to the MSC cultures.

### In Vivo Tumorogenic Assays

***Ectopic and Orthotopic Inoculations.*** NOD/SCID-IL2$\gamma R^{-/-}$ (NSG) immunodeficient mice were obtained from Jackson Laboratories (Bar Harbor, ME, http://www.jax.org). Mice were housed under specific pathogen-free conditions, fed ad libitum, and maintained under veterinary care according to animal welfare guidelines. Eight to ten weeks old mice were inoculated either subcutaneously (s.c.), intrabone (i.b.), or periosteally (p.). Prior to inoculation, cells were resuspended in Phosphate buffered saline (PBS) with or without 20 μg/mL BMP-2 (Noricum, Madrid, Spain, http://www.noricumimplants.com/) and filtered through a 70 μm nylon filter. For s.c. inoculation, $5 \times 10^6$ cells per mouse were injected under the skin in the flank of the mice. For the i.b. inoculation, mice were anesthetized with isoflurane, and the leg was bent 90° in order to drill the tip of the tibia with a 25G needle before cell inoculation ($2.5 \times 10^5$ cells per mouse) using a 27G needle. Mice were treated with Buprenorphine:Carprofen (0.1:5 mg/kg) right after inoculation and then 24 hours and 48 hours after. For p. inoculation, mice were anesthetized by intraperitoneal injection of xylacine (Rompun, Bayer, Leverkusen, Germany, http://www.animalhealth.bayer.com) and ketamine (Imalgene 1000, Merial, Barcelona, Spain, http://www.merial.es). Then, $1 \times 10^6$ cells per mouse were loaded in a syringe with a 26G needle which was inserted from proximal to distal site of the leg until it reached the diaphysis of tibia and following the tibial crest. Bone surface was scraped with the needle, and cells were deposited in the periosteal space. Animals were sacrificed when the tumors reached approximately 1 $cm^3$ or 6 months after inoculation. All animal research protocols were approved by the corresponding Institutional Animal Research Ethical Committees.

***Ceramic Implant Preparation and Implantation.*** 40 mg of HA/TCP powder (Biomatlante, Vigneux de Bretagne, France, http://www.biomatlante.com/), washed previously with 1 mL of Dulbecco's modified Eagle's medium (DMEM) medium, was mixed with $1 \times 10^6$ MSCs in 1 mL of DMEM medium. The mixture was spun down (1,000 rpm, 5 minutes), and the ceramic/MSCs mix was cultured overnight. Then, the culture medium was removed and 35 μL of a 1 μg/μL solution of BMP-2 reconstituted in culture medium, 30 μL of thrombin (Sigma, St. Louis, MO, http://www.sigmaaldrich.com) reconstituted in 2% $CaCl_2$, and 30 μL of fibrinogen (Sigma) reconstituted in water were added to the ceramic/MSC mix. Finally, the implant mixture was allowed to solidify for 30 minutes in cell culture conditions. For the s.c. implantation, mice were anesthetized by intraperitoneal injection of xylacine and ketamine, and the surgical areas were shaved and sterilized with 70% alcohol. Next, a dorsal incision in the skin was made and a pocket under cutaneous tissue was created. When the implant was stably placed, the wound was sutured.

### μCT Analysis

Formol fixed samples were imaged in a μCT system (eXplore Vista, GE Healthcare, Pittsburgh, PA, http://www3.gehealthcare.com) with an X-ray tube voltage of 50 kV and a current of 200 μA. The scanning angular rotation was 180°, the angular increment 0.40°, and the voxel resolution 50 μm. Datasets were reconstructed and segmented into binary images and 3D surface reconstructions were made using MicroView ABA 2.2 software (GE Healthcare).

### Histological Processing and Immunohistochemistry

Tumor samples were fixed in formol and when necessary decalcified with 4% clorhidric acid/4% formic acid for 3 days before being embedded in paraffin, cut into 4-μm sections, and subjected to hematoxylin and eosin (H&E) staining, Masson's tricrome (M-T) staining, or immunohistochemistry for GFP detection. For M-T staining, deparafined samples were stained with Harris' hematoxylin for 10 minutes. Then, samples were washed for 5 minutes in water, stained with Fuccina ponceau dye for 5 minutes, and washed with phosphomolibdic acid. Next, samples were stained with methyl violate dye for 5 minutes, and finally, dehydrated with increasing alcohols and xilol. Immunohistochemistry against GFP and Ki67 was performed using specific anti-GFP (1:100, Invitrogen, Paisley, U.K., http://www.invitrogen.com) and anti-Ki67 (1:100, Thermo Scientific, Waltham, MA, http://www.thermoscientific.com) antibodies, respectively, and a secondary anti-rabbit biotinylated antibody (1:500, Jackson ImmunoResearch, Newmarket, U.K., http://www.jacksonimmuno.com). Tumor grade was analyzed in H&E stained preparations using the French Federation of Comprehensive Cancer Centers (FNCLCC) grading system [39].

### Flow Cytometry and Cell Sorting

The immunophenotype of MSCs and tumor cell lines was determined by flow cytometry using fluorochrome-conjugated monoclonal antibodies anti-Sca-1, CD11b, CD14, CD29, CD44, and CD45 (BD Bioscience, Franklin Lakes, NJ, http://www.bdbiosciences.com) as described [37].

### Genomic PCR

Total DNA was extracted using the DNeasy Kit (Qiagen, Valencia, CA, http://www1.qiagen.com). 200 ng of DNA was used for each PCR reaction. PCR conditions were as follows: predenaturation at 94°C for 5 minutes followed by 29 cycles of denaturation at 94°C for 30 seconds, annealing at 62°C (for p53), 60°C (for RB), or 67°C (for $\beta$-actin) for 30 seconds and extension at 72°C for 50 seconds. Primer sequences used are shown in Supporting Information Table S1.

### Quantitative PCR

Total RNA was extracted from transformed MSCs and tumor-derived cell lines. cDNA synthesis was performed using the First-strand cDNA Synthesis Kit (GE Healthcare), and the expression of relevant genes was assessed by reverse transcriptase quantitative PCR (RT-qPCR) using SYBR Green PCR Kit (Qiagen) in untreated cells or in cells treated with BMP-2 (4 μg/mL), BMP-2 + DMH1 (R&D Systems, Minneapolis, MN, http://www.rndsystems.com) (0.5 μM) or BMP-2 + dickkopf one (DKK1) (R&D systems, Minneapolis, MN, http://www.rndsystems.com) (0.1 μg/mL). $\beta$-Actin was used as a housekeeping gene. The following PCR conditions were used: 5 minutes at 94°C, 35 cycles of 30 seconds at 94°C followed by 50 seconds at 60°C and 50 seconds at 72°C, and a final extension of 10 minutes at 72°C. Primer sequences are shown in Supporting Information Table S1. Statistical significance of the gene expression levels was analyzed using the Student's *t* test.

### Western Blot

Whole cell protein extraction and Western blot analysis were done as previously described [40] using anti-$\beta$-catenin (1:1,000, BD Bioscience) and anti-$\beta$-Actin (1:20,000, Sigma) primary antibodies.

### Measurement of Alkaline Phosphatase Activity

The activity of alkaline phosphatase (ALP) was evaluated through a colorimetric assay using cell lysates prepared after a 7-day treatment in the indicated conditions as previously described [41]. Total cellular protein content of cell lysates was determined using a Bradford assay (BioRad, Hercules, CA, http://www.bio-rad.com), and the ALP activity (O.D. 405 nm) per μg of total protein was represented.

## RESULTS

### Bone Environment Signals Redirect the Sarcomagenic Phenotype of p53$^{-/-}$ and p53$^{-/-}$RB$^{-/-}$ MSCs Toward OS Development

We have previously reported that Cre-mediated depletion of p53 and/or Rb in p53$^{loxP/loxP}$, RB$^{loxP/loxP}$, and p53$^{loxP/loxP}$RB$^{loxP/loxP}$ MSCs caused a significant increase in the proliferation and life span of mutant MSCs, and that p53- and p53/RB-deficient BM-MSCs or ASCs originate leiomyosarcoma-like tumors after s.c. inoculation into immunodeficient mice [22, 23]. We hypothesized that the bone microenvironment may play a role in regulating the osteogenic differentiation of transformed MSCs, and that intrabone (orthotopic) delivery of these transformed MSCs may impose an OS phenotype. To address this, GFP-tagged cultures of wt, p53$^{-/-}$, RB$^{-/-}$, and p53$^{-/-}$RB$^{-/-}$ BM-MSCs and ASCs [22, 23] were inoculated intratibia into NSG immunodeficient mice. As previously seen in s.c. inoculation experiments, only p53$^{-/-}$ and p53$^{-/-}$RB$^{-/-}$ BM-MSCs or ASCs developed tumors in vivo (Table 1). p53$^{-/-}$RB$^{-/-}$ MSCs displayed a higher tumor incidence and shorter latency than p53$^{-/-}$ MSCs (Table 1). Microcomputered tomography (μ-CT) analysis revealed the formation of tumors resembling human OS radiographic

**Table 1.** In vivo tumor formation ability of wt, $Rb^{-/-}$, $p53^{-/-}$, $Rb^{-/-}p53^{-/-}$ BM-MSCs/ASCs

| MSC type | Subcutaneous inoculation[a] | | | Intrabone inoculation | | | Periosteal inoculation | | |
|---|---|---|---|---|---|---|---|---|---|
| | Tumor incidence | Latency[b] | Histological analysis | Tumor incidence | Latency[b] | Histological analysis | Tumor incidence | Latency[b] | Histological analysis |
| BM-MSCs | | | | | | | | | |
| Wt | 0/8 | – | – | 0/5 | – | – | – | – | – |
| $Rb^{-/-}$ | 0/9 | – | – | 0/6 | – | – | – | – | – |
| $p53^{-/-}$ | 6/12 | 65–148 (107) | Leiomyosarcoma | 4/9 | 94–116 (105) | Osteosarcoma | 2/2 | (110) | Osteosarcoma |
| $Rb^{-/-}p53^{-/-}$ | 19/25 | 31–109 (65) | Leiomyosarcoma | 10/14 | 48–156 (93) | Osteosarcoma | 4/4 | 24–20 (22) | Osteosarcoma |
| ASCs | | | | | | | | | |
| Wt | 0/8 | – | – | 0/5 | – | – | – | – | – |
| $Rb^{-/-}$ | 0/8 | – | – | 0/5 | – | – | – | – | – |
| $p53^{-/-}$ | 4/8 | 43–123 (74) | Leiomyosarcoma | 5/9 | 126–173 (157) | Osteosarcoma | 1/4 | (120) | Osteosarcoma |
| $Rb^{-/-}p53^{-/-}$ | 7/13 | 43–69 (54) | Leiomyosarcoma | 7/9 | 100–174 (128) | Osteosarcoma | 6/6 | 63–90 (77) | Osteosarcoma |

[a]Data from Rubio et al., 2010 (ASCs) and Rubio et al., 2012 (BM-MSCs) [22, 23].
[b]Range of days needed to reach a tumor volume of 1 $cm^3$ (mean).
Abbreviations: ASCs, adipose-derived mesenchymal stem cells; BM-MSCs, bone marrow-derived mesenchymal stem cells; Wt, wild type.

features in the tibia of mice inoculated with $p53^{-/-}RB^{-/-}$ BM-MSCs or ASCs (Fig. 1A). These tumors displayed changes in the cortical bone intensity and mineralized osteoid both inside and outside of the bone [5]. H&E or M-T staining of tumors (Fig. 1B; Supporting Information Fig. S1) confirmed their resemblance with human OS (Supporting Information Fig. S2), including the presence of extensive areas of osteid matrix formed by spindle or polyhedral tumoral cells both inside (Fig. 1B-i, ii) and outside the host bone marrow cavity (Fig. 1B-i, iii, iv). These osteoid areas commonly display a lacy pattern, typical of osteoblastic OS, and are mainly formed by GFP+ cells, confirming their tumoral origin (Fig. 1B-iv, v). Likewise, the classical periosteal reaction to tumoral cells is also observed. The new formed reactive bone usually displayed the typical "sunburst" appearance (Fig. 1B-i, v; Supporting Information Fig. S1A-iii). Although the osteoblastic component was predominant, tumors derived from both p53- and p53RB-deficient BM-MSCs and ACSs also displayed areas of tumoral condroblastic differentiation (Fig. 1B-vi). Importantly, all these OS-related features were less evident or completely lost in the areas of the tumor distant from the recipient bone. Tumoral areas far from the host bone displayed a pathology resembling undifferentiated sarcomas mainly composed by interlacing fascicles of spindle cells, similar to the leiomyosarcoma-like tumors generated by these MSCs upon s.c. inoculation (Fig. 1B-vii). This indicates that the host bone environment seems to play an active role in programming the oncogenic potential/phenotype of transformed MSCs. The grading of a cohort of the tumors applying a three-grade system commonly used for sarcomas classification (FNCLCC system) [39] suggests that tumors derived from $p53^{-/-}$ or $p53^{-/-}RB^{-/-}$ BM-MSCs present higher mitotic counts and therefore higher grade than tumors derived from the corresponding ASC genotypes (Supporting Information Table S2).

The malignant nature of OS is evidenced by the appearance of metastasis. In our model, we detected GFP+ cells colonizing and metastasizing in lungs, spleen, and heart of different mice (Fig. 1C; Supporting Information Fig. S3). Importantly, all these distant metastasis presented extensive mineralized osteoblastic areas further evidencing the OS nature of the primary tumor (Supporting Information Fig. S3).

Although OS usually arises in the marrow cavity of long tubular bones, it also may arise on the surface of the bones [5]. Therefore, to investigate other orthotopic bone environments, GFP-tagged $p53^{-/-}$ and $p53^{-/-}RB^{-/-}$ BM-MSCs/ASCs were inoculated in the periosteal space of the tibia of immunodeficient mice. $p53^{-/-}RB^{-/-}$ MSCs also developed tumors with a shorter latency than $p53^{-/-}$ MSCs (Table 1). These tumors showed similar radiological (Fig. 2A; Supporting Information Fig. S4) and histological (Fig. 2B, 2C) OS-like features to those intratibia-formed tumors. Tumoral osteoid/chondroid areas adjacent to both the outer and the inner sides of the bone were evidenced by µ-CT analysis (Fig. 2A; Supporting Information Fig. S4) and H&E or M-T staining (Fig. 2B, 2C). These newly formed osteoid/chondroid areas comprises GFP+ cells confirming a tumoral MSC origin (Fig. 2B-iii, 2C-iii).

To further characterize these experimentally induced OS, primary tumors derived from $p53^{-/-}$ and $p53^{-/-}RB^{-/-}$ BM-MSCs as well as $p53^{-/-}$ ASCs were harvested, disaggregated, and placed back in MSC culture conditions to establish immortalized cell lines (TIB-BM-p53#1, TIB-BM-p53RB#1 to #3, and TIB-ASC-p53#1 to #3). As expected, these tumor cell lines remained deficient for p53 and RB (Fig. 3A) and displayed identical immunophenotype than their parental MSCs (Fig. 3B; Supporting Information Fig. S5) [22, 23]. Next, to further confirm the OS diagnosis of tumors at the molecular level, we analyzed the expression of several early (BMP-4 and Osterix) and late (Osteopontin and Osteocalcin) osteogenic markers in two TIB-BM-p53RB cell lines (Fig. 3C) and two TIB-ASC-p53 cell lines (Fig. 3D). All these osteogenic markers were upregulated in the TIB-BM-p53RB cell lines as compared to the parental BM-MSCs (BM-MSC-$p53^{loxP/loxP}RB^{loxP/loxP}$), and to a cell line derived from a leiomyosarcoma-like tumor formed upon s.c. inoculation of $p53^{-/-}RB^{-/-}$ BM-MSCs (T-BM-p53RB) (Fig. 3C). Similarly, these osteogenic markers were partially upregulated in TIB-ASC-p53 cell lines as compared to the parental ASCs (ASC-$p53^{loxP/loxP}$) (Fig. 3D). Together, these data indicate that environment signals provided by the bone milieu are able to redirect towards an OS development the otherwise leiomyosarcoma tumorogenic potential of p53/RB-deficient MSCs.

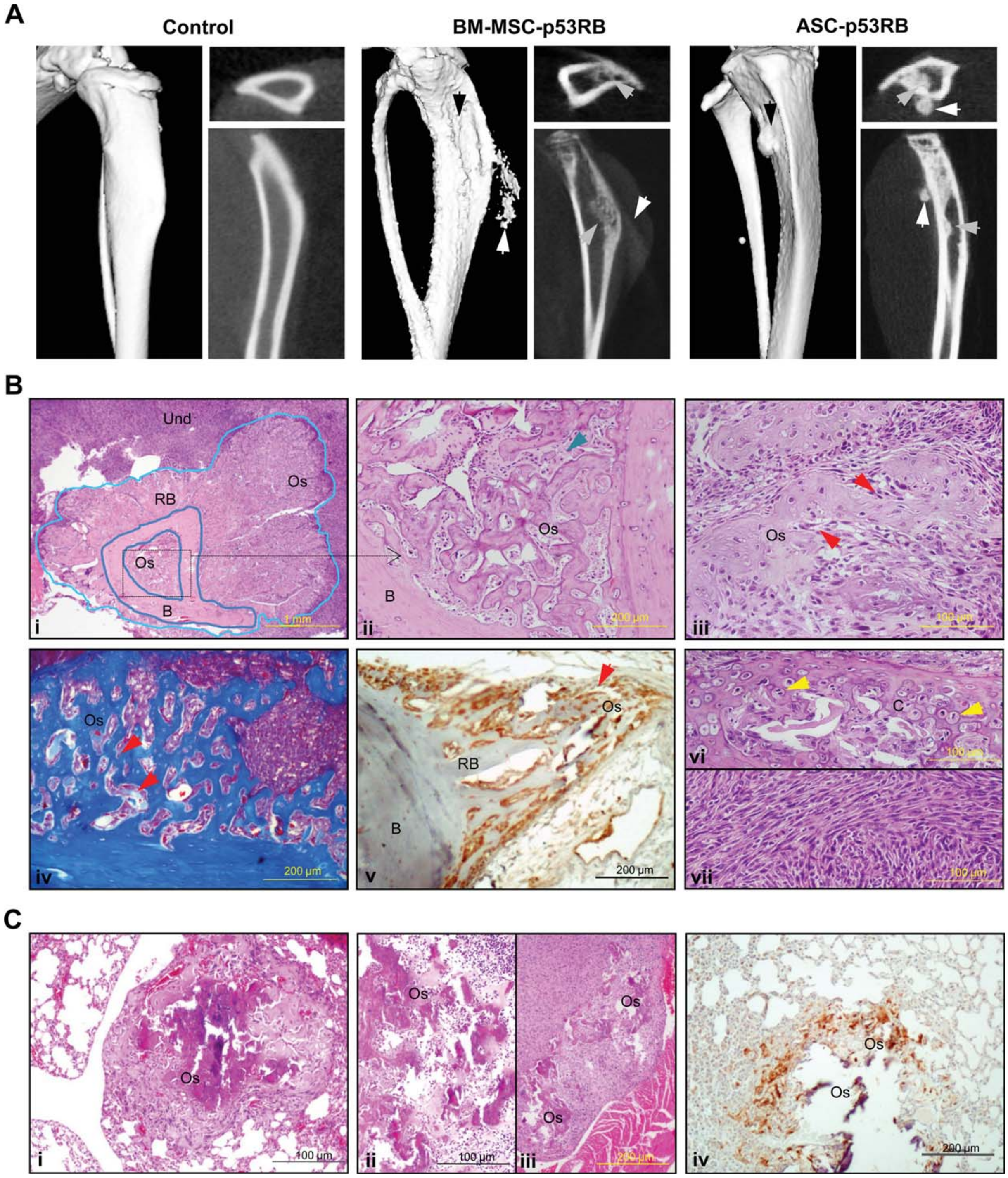


**Figure 1.** Development of osteosarcoma (OS) upon intrabone inoculation of p53−/− and p53−/−RB−/− BM-MSCs/ASCs. **(A):** Images of bone surface (isosurface; left panels) and representative sagital (right top panels) and longitudinal (right bottom panels) orthogonal images obtained by µ-CT of a control leg and legs intrabone inoculated with p53−/−RB−/− BM-MSCs or p53−/−RB−/− ASCs. Compared to the control leg, changes in cortical bone intensity (black arrows), diffuse peribone formation (white arrows), and intramarrow bone formation (gray arrows) resembles human OS features in legs inoculated with transformed MSCs. **(B):** Hematoxylin and eosin (H&E) staining (i–iii, vi–vii), Masson's tricrome staining (iv), and green fluorescent protein (GFP) immunostaining (v) of representative areas showing the main histological features of tumors arising in mice intrabone inoculated with either p53−/− or p53−/−RB−/− BM-MSCs/ASCs (Supporting Information Fig. S1 for cell type/genotype classified images). **(C):** H&E staining (i–iii) and GFP immunostaining (iv) of metastatic nodules showing osteogenic differentiation observed in the lung (i, iv), spleen (ii), and heart (iii) of mice intrabone inoculated with p53−/−RB−/− BM-MSCs. Normal recipient bone (B), reactive bone (RB), tumoral osteogenic areas (Os), chondroblastic areas (C), and tumoral undifferentiated areas (Und) are indicated. Blue arrows indicate the presence of osteogenic tumoral cells in the BM niche, yellow arrows indicate mitotic cells, and red arrows indicate the presence of osteoid matrix-forming tumoral cells. Blue lines were used to depict the border between host bone and ectopic tumor osteogenic areas. Abbreviations: ASC, adipose-derived MSCs; BM-MSC, bone marrow-derived MSC; B, normal recipient bone; C, chondroblastic area; MSC, mesenchymal stem cell; Os, tumoral osteogenic area; RB, reactive bone; Und, tumoral undifferentiated area.

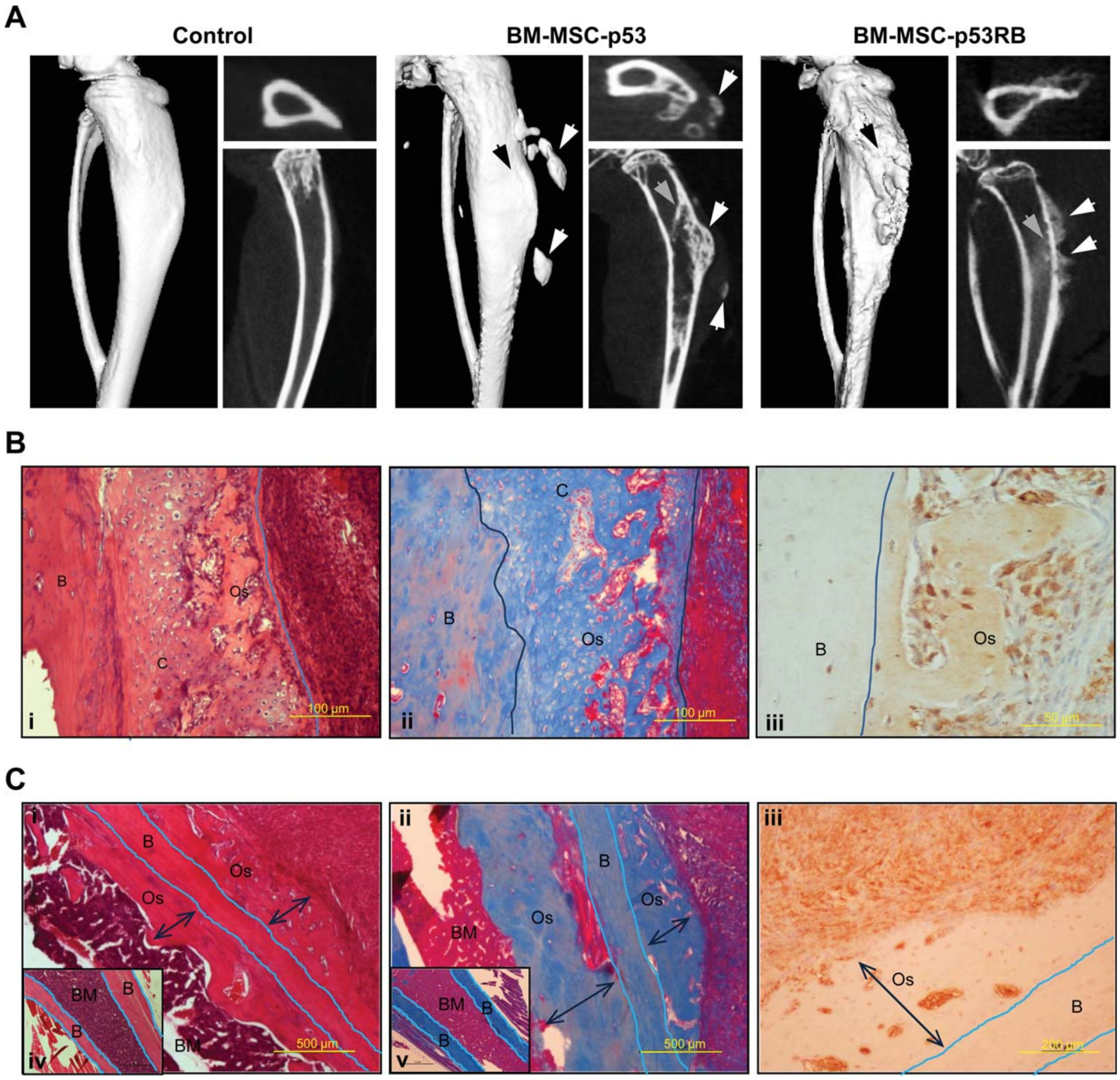


**Figure 2.** Development of osteosarcoma (OS) upon periosteal inoculation of p53−/− and p53−/−RB−/− BM-MSCs/ASCs. **(A):** Images of bone surface (isosurface; left panels) and representative sagital (right top panels) and longitudinal (right bottom panels) orthogonal images obtained by µ-CT of a control leg and legs periosteally inoculated with p53−/− or p53−/−RB−/− BM-MSCs. Compared to the control leg, changes in cortical bone intensity (black arrows), diffuse peribone formation (white arrows), and intra-marrow bone formation (gray arrows) resemble human OS features in legs inoculated with transformed MSCs. **(B, C):** Hematoxylin and Eosin (H&E) staining (i), Masson's tricrome (M-T) staining (ii), and green fluorescent protein (GFP) immunostaining (iii) of tumors formed upon periosteal inoculation of GFP-expressing p53−/−RB−/− BM-MSCs (B) and p53−/−RB−/−ASCs (C). H&E and M-T stainings are also shown as insets for noninoculated bones (C; iv, v). (M–T) staining was used to highlight areas of bone/cartilage and GFP detection was used to distinguish host bone (GFP−) from adjacent tumor-derived osteogenic areas (GFP+). Normal recipient bone (B), normal bone marrow (BM), tumoral osteogenic areas (Os), and tumoral chondrogenic areas (C) are indicated. Blue lines were used to depict the border between host bone and ectopic tumor osteogenic areas. Abbreviations: BM, bone marrow; MSC, mesenchymal stem cell; B, normal recipient bone; C, tumoral chondrogenic area; MSC, mesenchymal stem cell; Os, tumoral osteogenic area.

### BMP-2 Promotes Osteogenic Differentiation Through the Activation of WNT Signaling and Promotes OS Development from p53$^{-/-}$RB$^{-}$ MSCs with no Need of Orthotopic Inoculation

We have demonstrated that signals from the bone milieu induce in vivo osteogenic differentiation of transformed p53$^{-/-}$RB$^{-/-}$ BM-MSCs/ASCs and OS development. We next attempted to investigate the contribution of individual osteogenic factors. We first studied the response of p53$^{-/-}$RB$^{-/-}$ BM-MSCs/ASCs to treatment with media conditioned by confluent cultures of Saos-2 cells, a human osteosarcoma cell line with high osteoinductive ability [38]. We found that p53−/−RB−/− BM-MSCs/ASCs treated with Saos-2 conditioned medium displayed a significant increase in the osteoblastic-related ALP activity (Supporting Information Fig. S6). Since Saos-2 cells osteoinductive ability is highly dependent on the expression of osteogenic BMPs [38], we analyzed whether BMP-2 confers osteogenic differentiation potential to p53$^{-/-}$RB$^{-/-}$ BM-MSCs.

 

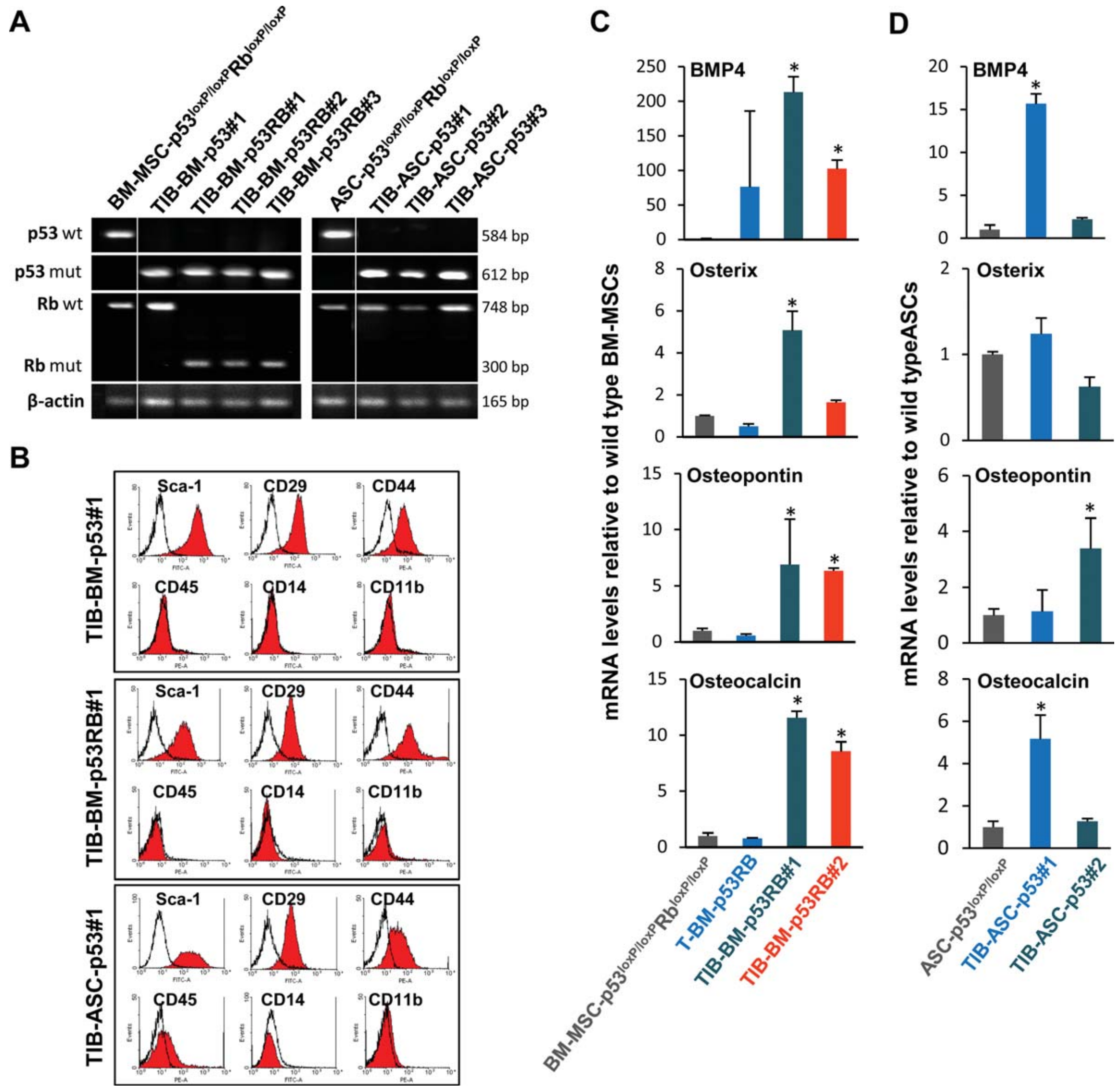


**Figure 3.** Immortalized cell lines ex vivo derived from primary osteosarcoma (OS) generated by tumorogenic p53- and p53/RB-deficient BM-MSCs/ASCs show a MSC phenotype and express osteogenic markers. **(A):** Genomic polymerase chain reaction (PCR) confirming that immortalized cell lines ex vivo-derived from primary OS tumors formed upon intrabone inoculation of p53−/− BM-MSCs (TIB-BM-p53), p53−/−RB−/− BM-MSCs (TIB-BM-p53RB), and p53−/− ASCs (TIB-ASC-p53) retained p53 and/or RB deficiency. **(B):** Immunophenotypic profile of the indicated tumoral cell lines analyzed by flow cytometry. Representative dot plots are shown for Sca-1, CD29, CD44, CD14, CD11b, and CD45. Empty lines represent the irrelevant isotypes. Red-filled lines display antibody-specific staining. **(C, D):** Reverse transcriptase quantitative PCRs showing the upregulation of the indicated osteogenic markers in two TIB-BM-p53RB cell lines as compared to either the original BM-MSC-p53$^{loxP/loxP}$RB$^{loxP/loxP}$ cells or to a cell line derived from a leiomyosarcoma-like tumor formed upon subcutaneous inoculation of p53−/−RB−/− BM-MSCs (T-BM-p53RB) (C), and in two TIB-ASC-p53 cell lines as compared to the original ASCs (ASC-p53$^{loxP/loxP}$) (D) *, $p < .05$ versus control cells. Abbreviations: ASC, adipose-derived MSCs; BMP, bone morphogenetic protein; BM-MSC, bone marrow-derived MSC; MSC, mesenchymal stem cell; wt, wild type.

BMP-2 was able to induce the expression of early (Osterix and ALP) and late (Osteocalcin) osteogenic markers which was reversed by DMH1, a selective inhibitor of the type I BMP receptors (BMPR-I) [42] that mediate the BMP-2-induced osteblastic signals in MSCs [43] (Fig. 4A).

It was reported that the pro-osteogenic effect of BMP-2 on pre-osteoblastic cells is mediated through the BMP-2-induced activation of WNT signaling [44]. We thus investigated whether WNT signaling is also relevant in the BMP-2-induced osteogenic differentiation of transformed MSCs. We found that treatment of p53$^{-/-}$RB$^{-/-}$ BM-MSCs with BMP-2 resulted in a 20-fold upregulation of the canonical WNT signaling activator WNT3A that was fully reversed by the BMPR-I inhibitor DMH1 (Fig. 4B). Likewise, BMP2 treatment increased intracellular levels of key WNT signaling mediator $\beta$-catenin (Fig. 4C). The WNT signaling inhibitor DKK1 prevented $\beta$-catenin accumulation (Fig. 4C) and was able to almost completely block the BMP-2-induced expression of osteogenic markers (Fig. 4A) suggesting that BMP-2 induces osteogenic differentiation of transformed MSCs through the regulation of WNT signaling.

After confirming the osteogenic effect of BMP-2 in vitro, we studied whether BMP-2 also confers in vivo osteogenic differentiation potential and promotes OS development from

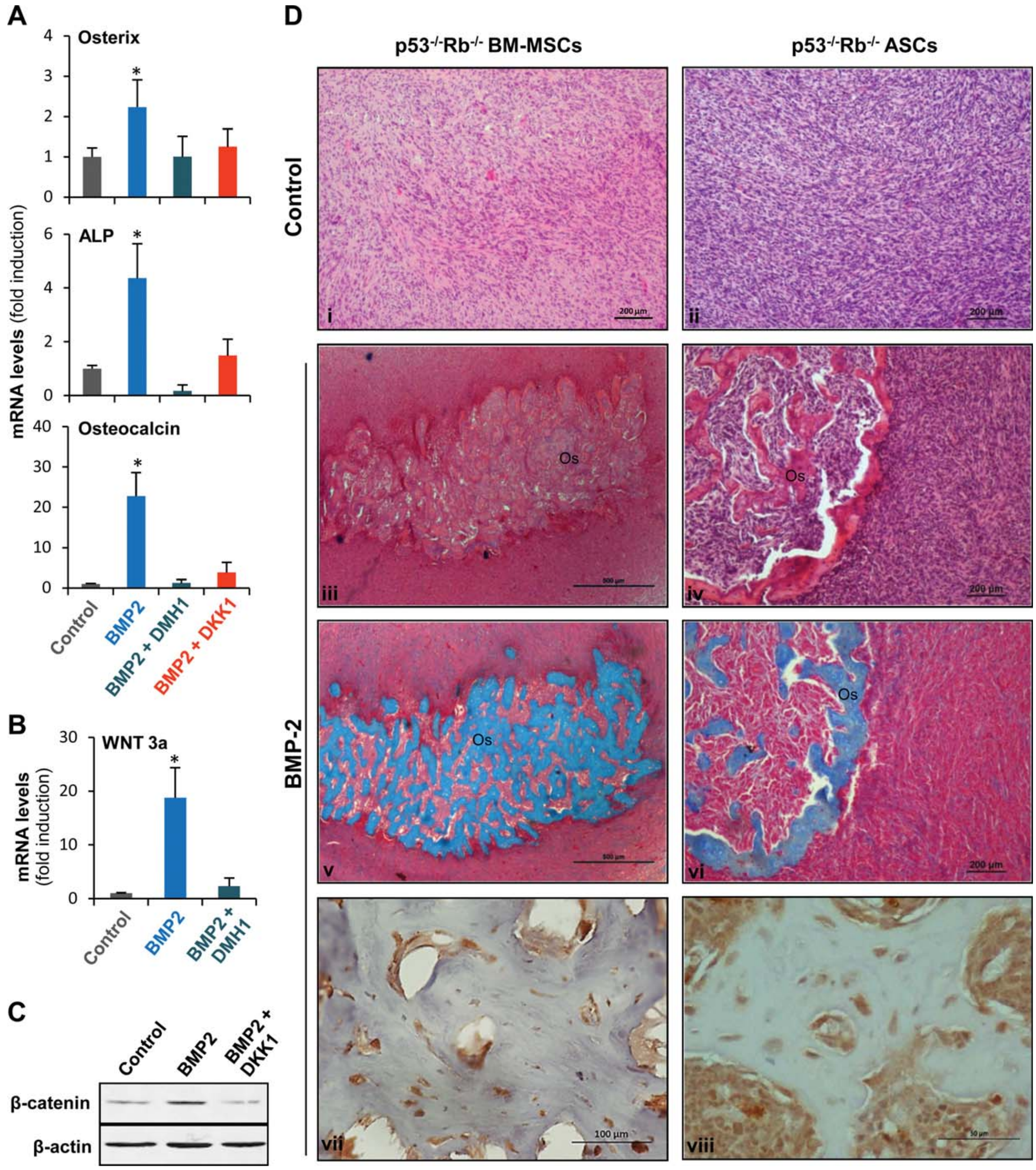


**Figure 4.** BMP-2 administration promotes osteogenic differentiation through the activation of Wnt singnaling and OS development upon subcutaneous inoculation. **(A, B):** Reverse transcriptase quantitative polymerase chain reaction (RT-qPCRs) showing the relative mRNA expression levels of the indicated osteogenic markers (A) or WNT3A (B) upon treatment of p53−/−RB−/− BM-MSCs with BMP-2 (4 μg/mL), BMP-2 + DMH1 (0.5 μM), or BMP-2 + DKK1 (0.1 μg/mL) for 5 days *, $p < .05$ versus control cells. **(C):** Western blotting showing the expression of $\beta$-catenin protein in p53−/−RB−/− BM-MSCs after a 24 hours-treatment with BMP-2 or BMP-2 + DKK1. The expression of $\beta$-actin was used as loading control. **(D):** Hematoxylin and eosin staining (i–iv), Masson's tricrome staining (v, vi), and green fluorescent protein (GFP) immunostaining (vii, viii) of tumors formed upon subcutaneous inoculation of GFP-expressing p53−/−RB−/− BM-MSCs or p53−/−RB−/− ASCs implanted without (i, ii) or with 40 μg of BMP-2 (iii–viii). Tumoral osteogenic areas (Os) are indicated. Scale bars = 500 μm (iii and v); 200 μm (i, ii, iv, and vi); 100 μm (vii); and 50 μm (viii). Abbreviations: ALP, alkaline phosphatase; ASCs, adipose-derived MSCs; BMP, bone morphogenetic protein; BM-MSCs, bone marrow-derived MSCs; DKK1, dickkopf one; MSCs, mesenchymal stem cells; Os, tumoral osteogenic areas.

GFP-tagged p53$^{-/-}$RB$^{-/-}$ BM-MSCs/ASCs delivered via s.c. into immunodeficient mice. Both control- and BMP-2-treated p53$^{-/-}$RB$^{-/-}$ BM-MSCs and ASCs developed tumors with similar penetrance and latency (Table 2). As previously reported [22, 23], tumors developed from control-treated p53$^{-/-}$RB$^{-/-}$ BM-MSCs/ASCs resembled leiomyosarcomas and did not show evidence of osteogenic differentiation (Fig. 4D). However, tumors developed from both p53$^{-/-}$RB$^{-/-}$

 

**Table 2.** In vivo tumor formation ability of $Rb^{-/-}p53^{-/-}$ BM-MSCs/ASCs inoculated subcutaneously with BMP2 and using or not ceramic-fibrin-based implants

| MSC type | Treatment | s.c. inoculation | | | Ceramic implant | | |
|---|---|---|---|---|---|---|---|
| | | Tumor incidence | Latency[b] | Osteoid in tumors[a] | Tumor incidence | Latency[b] | Osteoid in tumors[a] |
| BM-MSC-$Rb^{-/-}p53^{-/-}$ | Control | 3/3 | 47 | – | 5/5 | 24 | + (next to ceramic) |
| | BMP2 | 3/3 | 47 | ++ (throughout tumor) | 5/5 | 24 | +++ (throughout tumor) |
| ASC-$Rb^{-/-}p53^{-/-}$ | Control | 3/4 | 57 | – | 8/8 | 53 | + (next to ceramic) |
| | BMP2 | 3/3 | 39 | ++ (throughout tumor) | 7/7 | 55 | +++ (throughout tumor) |

[a]Approximate extension and distribution pattern of osteoid areas in osteosarcomas based on histological analysis and referred to the total area of the tumor: –, no osteoid observed; +, less than 5%; ++, 5–15%; +++, more than 15%.
[b]Mean of days needed to reach a tumor volume of 1 $cm^3$
Abbreviations: ASCs, adipose-derived mesenchymal stem cells; BM-MSCs, bone marrow-derived mesenchymal stem cells; BMP, bone morphogenetic protein

BM-MSCs and $p53^{-/-}RB^{-/-}$ ASCs s.c. inoculated with BMP-2 displayed extended areas of osteoid matrix (Fig. 4D). Importantly, these bone-forming areas were GFP+, confirming that they developed from the BMP-2-stimulated $p53^{-/-}RB^{-/-}$ MSCs (Fig. 4D). These data support the ability of BMP-2 to induce osteogenic differentiation of transformed MSCs in vivo and to contribute to the acquisition of the OS phenotype in an ectopic (s.c.) environment.

### Calcified Substrates Induce In Vivo Osteogenic Differentiation of $p53^{-/-}RB^{-/-}$ MSCs and Synergistically Cooperate with BMP-2 in OS Development

Apart from individual osteogenic factors present in the bone milieu, like BMP-2, the calcified extracellular matrix is another key environmental factor supposed to play a role in osteogenic differentiation [33, 34]. To test the osteoinductive ability of the calcified extracellular matrix alone or in combination with BMP-2, we prepared pellets of $p53^{-/-}RB^{-/-}$ BM-MSCs/ASCs containing or not HA/TCP as calcified substrate and cultured them in the presence or absence of BMP-2. Consistent with the BMP-2-induced expression of the ALP gene (Fig. 4A), we observed an increase in ALP activity in BMP-2-treated $p53^{-/-}RB^{-/-}$ BM-MSCs/ASCs (Fig. 5A). On the other hand, cells embedded in HA/TCP alone displayed only a modest gain in ALP activity, although the combination of both HA/TCP ceramic and BMP-2 synergistically increased ALP activity (Fig. 5A). To test the role of calcified substrates and BMP-2 combination in OS development in vivo, we devised ceramic implants composed of HA/TCP, GFP-expressing $p53^{-/-}RB^{-/-}$ BM-MSCs/ASCs, and a fibrin coating to facilitate their s.c. implantation into immunodeficient mice (Fig. 5B). Both control (culture medium) and BMP-2 loaded implants developed tumors with similar latencies (Table 2). Importantly, tumors developed in the absence of BMP-2 showed small areas of osteogenic differentiation only surrounding the ceramic material (Fig. 5C, 5D). However, when BMP-2 was incorporated to the ceramic-fibrin structure, tumors containing large areas of GFP+ tumorogenic osteoid matrix, spread throughout the tumor and resembling the lace-like pattern typical of human OS, were developed (Fig. 5C, 5D). All tumors showed abundant proliferating cells (nuclear Ki67 staining) both in undifferentiated areas and in the surroundings of osteoid-differentiated areas and the presence of BMP-2 or calcified substrates did not seem to influence the proliferation index (Supporting Information Fig. S7).

These results suggest a relevant role for bone milieu signals in the development of the OS phenotype from $p53^{-/-}RB^{-/-}$ transformed MSCs. This HA/TCP-based ceramic/fibrin bone-like environment model represents a powerful system for testing potential individual factors/molecules involved in OS pathogenesis as well as novel therapeutic compounds.

## Discussion

Cancer-specific hallmark oncogenic hits must arise in the appropriate target cell (the so-called tumor initiating cell, TIC) in order to initiate an oncogenic process [45]. However, increasing evidence supports a relevant role of the cellular microenvironment in regulating both stem cell fate and cancer cell growth [46–48]. Cell-cell contact interactions and paracrine soluble factors may influence the tumor phenotype and evolution [45, 48]. Thus, in vivo models capable of integrating both the nature of the target cell for transformation, the underlying oncogenic lesions, and the influence of the microenvironment will constitute a valuable model to study tumor biology and to assess potential novel therapeutic approaches [48].

Solid evidence indicates that MSCs and/or MSC-derived progenitors represent the TIC for human sarcomas [1–4]. Likewise, normal, nonmalignant MSC-like cells have been isolated at high frequencies from primary OS samples, suggesting that normal MSCs could be recruited to the microenvironment of OS and play a role in the development of the disease [49]. p53 and RB are master cell cycle regulators related with MSC differentiation [12–17] and loss-of-function mutations in p53 and/or RB are common in sarcomas, especially in OS, suggesting a relevant role for p53/RB deficiency as OS-driving mutations [6, 10, 11]. We have previously reported that p53 and RB inactivation in undifferentiated BM-MSCs or ASCs induces leiomyosarcoma upon s.c inoculation into immunodeficient mice [22, 23]. Conversely, p53 and RB inactivation in BM-MSC-derived osteogenic progenitors efficiently promoted the development of OS upon s.c. inoculation, whereas $p53^{-/-}RB^{-/-}$ ASC-derived osteogenic progenitors did not display tumorogenic potential [23]. These data indicate that the differentiation stage of BM-MSCs may impose the tumor phenotype. However, mouse models in which p53/RB were mutated in early mesenchymal progenitors of embryonic limb buds also developed OS [15, 21], suggesting that undifferentiated MSCs could also constitute the cell of origin for OS under certain osteogenic-inductive signals. In this regard, the expression

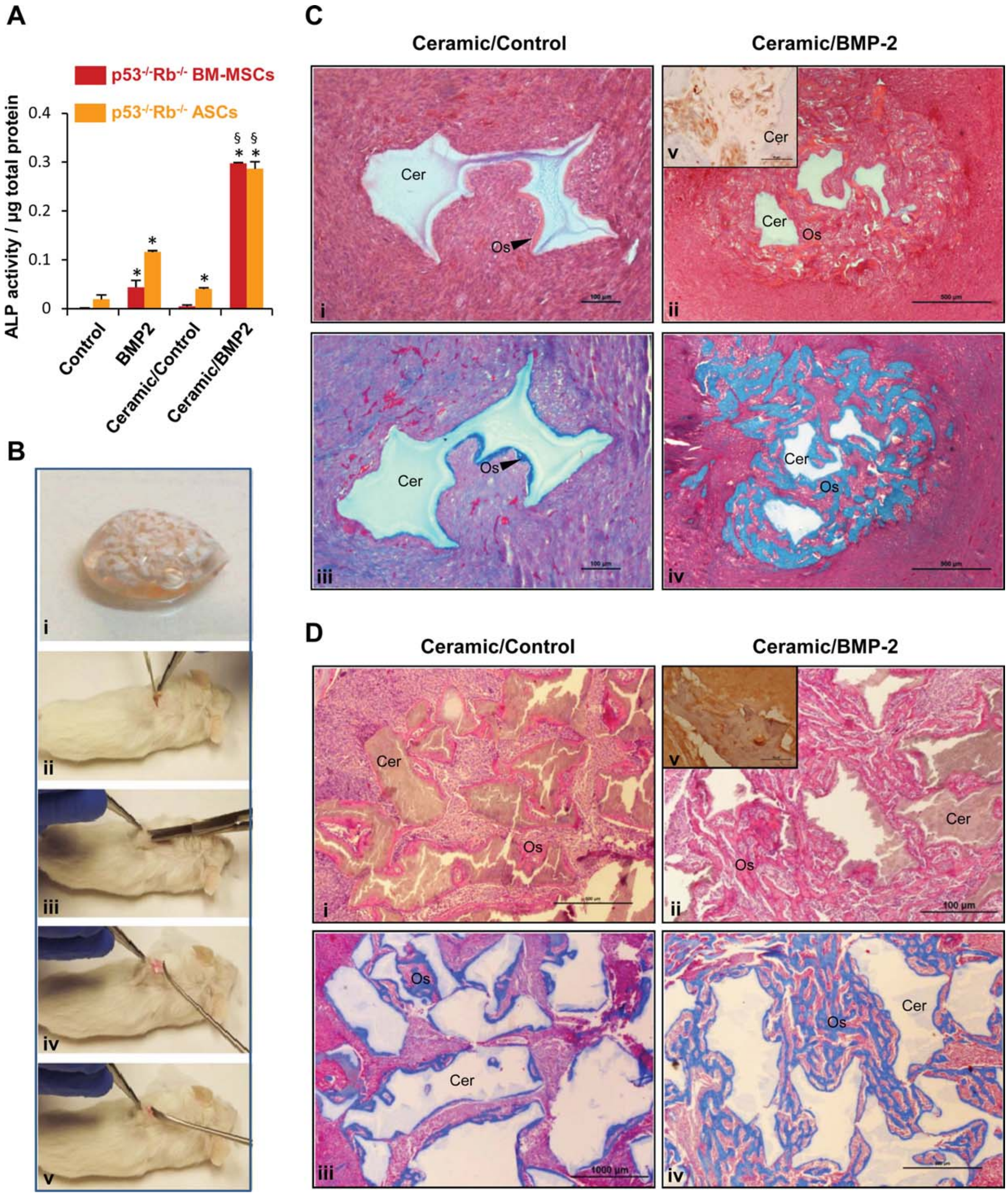


**Figure 5.** A ceramic bone-like environment model allows testing of individual bone factors involved in osteosarcoma (OS) development. **(A):** ALP activity per µg of protein in lysates of p53$^{-/-}$RB$^{-/-}$ BM-MSCs/ASCs pellets containing or not hydroxyapatite and tricalciumphosphate after a 7-day treatment with or without BMP-2 (4 µg/mL) as indicated *, $p < .05$ versus control cells; $^{§}$, $p < .05$ versus BMP-2 treated cells. **(B):** 40 mg of ceramic-fibrin based implants were used as carrier of tumoral cells and BMP-2. A representative implant (i) and a schematic sequence of the inoculation process (ii–v) are shown. **(C, D):** Hematoxylin and eosin staining (i, ii), Masson's tricrome staining (iii, iv), and green fluorescent protein (GFP) immunostaining (v) of tumors formed upon subcutaneous inoculation of ceramic implants containing GFP-expressing p53−/−RB−/− BM-MSCs (C) or p53−/−RB−/− ASCs (D) with or without 40 µg of BMP-2 as indicated. Ceramic pieces (Cer) and tumoral osteogenic areas (Os) are indicated. Scale bars = 100 µm (C-i, C-iii, D-i, and D-ii); 500 µm in (C-ii, C-iv, and D-iv); and 1,000 µm (D-iii). Abbreviations: ALP, alkaline phosphatase; ASCs, adipose-derived MSCs; BMP, bone morphogenetic protein; BM-MSCs, bone marrow-derived MSCs; Cer, ceramic pieces; MSCs, mesenchymal stem cell; Os, tumoral osteogenic areas.

of c-MYC in p16$^{INK4A-/-}$p19$^{ARF-/-}$ undifferentiated BM-MSCs resulted in OS development [50]. Additionally, similar gene expression signatures were found between human OS samples and undifferentiated MSCs or osteogenic-committed MSCs [51], suggesting that OS may develop in osteogenic progenitors or in undifferentiated MSCs.

To address whether the bone environment influences the in vivo differentiation and the sarcomagenic potential of transformed MSCs, $p53^{-/-}$ and $p53^{-/-}RB^{-/-}$ BM-MSCs, and ASCs were inoculated either intrabone or in periosteum. Orthotopic inoculation of these transformed undifferentiated MSCs consistently generated osteoblastic OS displaying human OS radiographic and histological features, including extensive areas of tumoral osteoid matrix. The osteogenic ability of the transformed MSCs was further evidenced by their infiltration (metastasis presenting osteoid areas) in lung, spleen, and heart. Moreover, ex vivo tumoral cell lines derived from primary tumors displayed upregulation of early and late osteogenic markers. Together, these data demonstrate that bone environment signals play a role in osteogenic differentiation and sarcomagenesis by defining the sarcoma phenotype regardless the source of the MSCs. Therefore, either BM-MSC-derived osteogenic progenitors or undifferentiated BM-MSCs/ASCs may represent of OS-TIC under the proper microenvironment signals. It might be speculated that the more differentiated the target cell for transformation is, the more differentiated the resulting OS would be [4, 6, 23]. Notably, the histological OS features became less evident in areas distant from the host bone, further highlighting the role of microenvironment signals in osteogenic differentiation. In line with this, a recent characterization of 19 OS cell lines found that half of them were unable to generate tumors after ectopic inoculation into immunodeficient mice and the remaining cell lines generated tumors classified as high-grade sarcomas displaying only a discrete osteogenic differentiation [52].

We have previously reported that gene expression profiling of BM-MSCs differentiated along the osteoblastic lineage before Cre-mediated deletion of p53 and RB, which generate OS after s.c. inoculation into inmunedeficient mice, showed alterations in several signaling pathways related to osteogenic differentiation and OS development, like those controlled by WNT (including the regulation mediated by WNT3A), calcium, and BMPs [23]. Therefore, we next wanted to study the individual contribution of master bone microenvironment factors such as BMP-2, WNT signaling, and calcified substrates to OS development. BMP-2 is expressed in human OS [53], and its role in OS development has been addressed in OS cell lines but not in primary transformed MSCs. We show that BMP-2 treatment enhances the expression of osteogenic markers in transformed MSCs. Likewise, BMP-2 is able to effectively induce in vivo osteogenic differentiation and OS development upon ectopic s.c inoculation of $p53^{-/-}RB^{-/-}$ BM-MSCs and ASCs without significant differences in tumor latency, thus mimicking the effects observed upon orthotopic inoculation of $p53^{-/-}RB^{-/-}$ BM-MSCs/ASCs. Previous work on OS cell lines revealed controversial effects of BMP-2 on osteogenic differentiation and tumor growth. It has been reported that BMP-2 failed to induce bone formation from human OS cell lines that harbor differentiation defects and instead efficiently promote tumor growth [54]. Conversely, it has been shown that BMP-2 treatment of a TIC population isolated from human OS cell lines induced the upregulation of terminal osteogenic markers inhibiting their tumorogenic potential [55]. These controversial data on genomically unstable transformed OS cell lines pinpoints the need to study differentiation and transformation processes using primary MSCs harboring defined oncogenic lesions.

A previous report has shown that BMP-2 controls important features of MSC osteoblastic differentiation though the autocrine activation of WNT ligands like WNT1 and WNT3A [44]. Likewise, it was suggested that osteoblasts exert a direct control of osteogenic lineage commitment of mesenchymal progenitors through WNT singnaling-activating ligands, including WNT3A which is able to stimulate osteogenesis [56]. Similarly, we show that BMP-2 induces the expression of WNT3A and the accumulation of $\beta$-catenin in transformed MSCs and that the BMP-2-induced upregulation of osteogenic markers is blocked by the WNT signaling antagonist DKK1. In addition, coculture of transformed MSCs with and osteoinductive cell type such as Saos-2 cells [38] is able to significantly increase ALP activity. Altogether, it may be speculated that osteoinductive cell types present in the tumor microenviroment (both from host or tumoral origin) could produce osteogenic factors such as BMP-2 which in turn activated WNT signaling in transformed MSCs, thus contributing to OS phenotype development.

Calcium phosphate biomaterials, such as HA/TCP, are extensively used as a calcified scaffold to support in vivo the proliferation and differentiation of MSCs in degenerative or damaged osteoarticular conditions [33–35, 57]. We have recently set up a model to assess the in vivo differentiation potential of hMSCs based on s.c implantation into immunodeficient mice of hMSCs embedded in a fibrin-coated HA/TCP ceramic and supplemented with BMP-2 [58]. Here, we took advantage of this optimized ceramic model to analyze the effect of calcified substrates on the osteogenic differentiation and sarcomagenesis potential of $p53^{-/-}RB^{-/-}$ MSCs. Both $p53^{-/-}RB^{-/-}$ BM-MSCs and ASCs embedded in the fibrin-coated HA/TCP ceramic in the absence of BMP-2 developed tumors showing discrete areas of osteogenic differentiation surrounding the ceramic material, similar to previous studies using wt MSCs [33, 59]. However, the addition of BMP-2 displayed a synergistic effect along with HA/TCP calcified substrate resulting in OS development with extensive tumoral osteoid matrix distributed throughout the tumor. These results further highlight the importance of bone environment signals, such as calcium substrates and BMP-2, in programming the sarcomagenic potential of transformed $p53^{-/-}RB^{-/-}$ BM-MSCs/ASCs. Importantly, tumors developed from $p53^{-/-}RB^{-/-}$ BM-MSCs and ASCs in the ceramic/BMP-2 model exclusively displayed osteogenic differentiation and subsequent OS development, and no other mesenchymal tissue differentiation was found as it was observed when healthy hMSCs were inoculated [58]. This indicates that deficiency of p53 and RB predisposes BM-MSCs and ASCs toward the osteogenic lineage, thus favoring OS development.

It is worth mentioning that human cells are more resistant to undergo tumoral transformation than mouse cells, thus supporting the safety use of hMSCs in clinical applications. In this regard, hMSCs deficient for p53 and/or Rb failed to induce tumor formation in vivo [37, 60] suggesting that in the human setting additional cooperating mutations are needed to initiate sarcomagenesis [4, 60]. Nevertheless, it is plausible that microenvironment signals described in this work as able to influencing sarcoma formation from mMSCs are likewise relevant for modulating human sarcomagenesis.

## Conclusion

In summary, OS development is closely linked to MSC differentiation [6] and several key factors underlie its phenotype: (a) the acquisition of relevant oncogenic lesions favoring the growth advantage of tumor cells predisposed towards the osteogenic lineage; (b) the differentiation stage of MSCs toward osteogenic lineage; and (c) the influence of bone microenvironment proliferative and differentiation signals. Here, we have developed an osteoblastic OS model based on the integration of potential OS-TIC (BM-MSCs/ASCs), OS-predisposing oncogenic lesions (p53/RB deficiency), and the influence of bone microenvironment signals (calcified substrates and BMP-2). In contrast to existing OS models based on the ectopic or orthotopic inoculation of OS established cell lines into immunodeficient mice, this model is developed from the putative OS TIC, is easier to handle than orthotopic inoculations and is suitable for the study of the impact of individual milieu signals in physiological and pathological osteogenesis, eventually representing a valid model to assess the pre-clinical efficacy of novel OS therapeutic strategies.

## Acknowledgments

This work was supported by the Instituto de Salud Carlos III/ Fondos FEDER (PI10/00449 to P.M, PI11/00377FIS to J.G-C, CP11/00024 to R. Rodriguez), Tercel (RD12/0019/0006) and RTICC (RD12/0036/0015 and RD12/0036/0027); the Junta de Andalucia/FEDER (P08-CTS-3678 to P.M.), the MINECO (PLE-2009-0111 to P.M.), The Spanish Association Against Cancer (Junta Provincial de Albacete-CI110023 to P.M.), Grupo Espaol de Investigación en Sarcomas (beca J.M. Buesa-2012 to R. Rodriguez), Obra Social Cajastur-IUOPA, EuroNanomed ERA-NET initiative (REBONE project; PI10/02985FIS to J.G-C.), Comunidad de Madrid (CellCAM; P2010/BMD-2420 to J.G-C.) and Health Canada (H4084–112281 to P.M., R. Rodriguez, and M.R-M). R. Rodriguez and A. Abarrategi are supported, respectively, by the Miguel Servet and Sara Borrell programs of the ISCIII/FEDER. R. Rubio was supported by a fellowship of the ISCIII/FEDER. P.M. is an ICREA Professor supported by the Generalitat of Catalunya.

## Author Contributions

R. Rubio and A. Abarrategi: development of methodology, acquisition, analysis, and interpretation of data, and manuscript writing; L.M-C: acquisition, analysis, and interpretation of data; C.S., J.T., L.S., A. Astudillo, I.C., F.M., and M.R-M: analysis and interpretation of data; J.G-C.: development of methodology, conception and design, analysis and interpretation of data, financial support, and manuscript writing; P.M and R. Rodriguez: conception and design, analysis and interpretation of data, financial support, and manuscript writing. The manuscript has been seen and approved by all authors. P.M. and R. Rodriguez share senior authorship. R. Rubio, A. Abarrategi, and J.G.-C. contributed equally to this article.

## Disclosure of Potential Conflicts of Interest

The authors indicate no potential conflicts of interest.

## References

1 Abarrategi A, Marinas-Pardo L, Mirones I et al. Mesenchymal niches of bone marrow in cancer. Clin Transl Oncol 2011;13: 611–616.

2 Garcia-Castro J, Trigueros C, Madrenas J et al. Mesenchymal stem cells and their use as cell replacement therapy and disease modelling tool. J Cell Mol Med 2008;12: 2552–2565.

3 Rodriguez R, Garcia-Castro J, Trigueros C et al. Multipotent mesenchymal stromal cells: Clinical applications and cancer modeling. Adv Exp Med Biol 2012;741:187–205.

4 Rodriguez R, Rubio R, Menendez P. Modeling sarcomagenesis using multipotent mesenchymal stem cells. Cell Res 2012;22: 62–67.

5 Klein MJ, Siegal GP. Osteosarcoma: Anatomic and histologic variants. Am J Clin Pathol 2006;125:555–581.

6 Tang N, Song WX, Luo J et al. Osteosarcoma development and stem cell differentiation. Clin Orthop Relat Res 2008;466:2114–2130.

7 Helman LJ, Meltzer P. Mechanisms of sarcoma development. Nat Rev Cancer 2003; 3:685–694.

8 Malkin D, Li FP, Strong LC et al. Germ line p53 mutations in a familial syndrome of breast cancer, sarcomas, and other neoplasms. Science 1990;250:1233–1238.

9 Ng AJ, Mutsaers AJ, Baker EK et al. Genetically engineered mouse models and human osteosarcoma. Clin Sarcoma Res 2012;2:19.

10 Overholtzer M, Rao PH, Favis R et al. The presence of p53 mutations in human osteosarcomas correlates with high levels of genomic instability. Proc Natl Acad Sci USA 2003;100:11547–11552.

11 Wadayama B, Toguchida J, Shimizu T et al. Mutation spectrum of the retinoblastoma gene in osteosarcomas. Cancer Res 1994;54:3042–3048.

12 Lengner CJ, Steinman HA, Gagnon J et al. Osteoblast differentiation and skeletal development are regulated by Mdm2-p53 signaling. J Cell Biol 2006;172:909–921.

13 Tataria M, Quarto N, Longaker MT et al. Absence of the p53 tumor suppressor gene promotes osteogenesis in mesenchymal stem cells. J Pediatr Surg 2006;41:624–632; discussion 624–632.

14 Molchadsky A, Shats I, Goldfinger N et al. p53 plays a role in mesenchymal differentiation programs, in a cell fate dependent manner. Plos One 2008;3:e3707.

15 Calo E, Quintero-Estades JA, Danielian PS et al. Rb regulates fate choice and lineage commitment in vivo. Nature 2010;466:1110–1114.

16 De Falco G, Comes F, Simone C. pRb: Master of differentiation. Coupling irreversible cell cycle withdrawal with induction of muscle-specific transcription. Oncogene 2006;25:5244–5249.

17 Gutierrez GM, Kong E, Sabbagh Y et al. Impaired bone development and increased mesenchymal progenitor cells in calvaria of RB1−/− mice. Proc Natl Acad Sci USA 2008; 105:18402–18407.

18 Thomas DM, Carty SA, Piscopo DM et al. The retinoblastoma protein acts as a transcriptional coactivator required for osteogenic differentiation. Mol Cell 2001;8:303–316.

19 Berman SD, Calo E, Landman AS et al. Metastatic osteosarcoma induced by inactivation of Rb and p53 in the osteoblast lineage. Proc Natl Acad Sci USA 2008;105:11851–11856.

20 Walkley CR, Qudsi R, Sankaran VG et al. Conditional mouse osteosarcoma, dependent on p53 loss and potentiated by loss of Rb, mimics the human disease. Genes Dev 2008; 22:1662–1676.

21 Lin PP, Pandey MK, Jin F et al. Targeted mutation of p53 and Rb in mesenchymal cells of the limb bud produces sarcomas in mice. Carcinogenesis 2009;30: 1789–1795.

22 Rubio R, Garcia-Castro J, Gutierrez-Aranda I et al. Deficiency in p53 but not retinoblastoma induces the transformation of mesenchymal stem cells in vitro and initiates leiomyosarcoma in vivo. Cancer Res 2010;70: 4185–4194.

 

**23** Rubio R, Gutierrez-Aranda I, Saez-Castillo AI et al. The differentiation stage of p53-Rb-deficient bone marrow mesenchymal stem cells imposes the phenotype of in vivo sarcoma development. Oncogene 2013;32: 4970–4980.
**24** Chen G, Deng C, Li YP. TGF-beta and BMP signaling in osteoblast differentiation and bone formation. Int J Biol Sci 2012;8: 272–288.
**25** Luu HH, Song WX, Luo X et al. Distinct roles of bone morphogenetic proteins in osteogenic differentiation of mesenchymal stem cells. J Orthop Res 2007;25:665–677.
**26** Anderson HC, Hodges PT, Aguilera XM et al. Bone morphogenetic protein (BMP) localization in developing human and rat growth plate, metaphysis, epiphysis, and articular cartilage. J Histochem Cytochem 2000;48:1493–1502.
**27** Bais MV, Wigner N, Young M et al. BMP2 is essential for post natal osteogenesis but not for recruitment of osteogenic stem cells. Bone 2009;45:254–266.
**28** Tsuji K, Bandyopadhyay A, Harfe BD et al. BMP2 activity, although dispensable for bone formation, is required for the initiation of fracture healing. Nat Genet 2006;38:1424–1429.
**29** Bandyopadhyay A, Tsuji K, Cox K et al. Genetic analysis of the roles of BMP2, BMP4, and BMP7 in limb patterning and skeletogenesis. Plos Genet 2006;2:e216.
**30** Noel D, Gazit D, Bouquet C et al. Short-term BMP-2 expression is sufficient for in vivo osteochondral differentiation of mesenchymal stem cells. Stem Cells 2004;22:74–85.
**31** Gautschi OP, Frey SP, Zellweger R. Bone morphogenetic proteins in clinical applications. Ann J Surg 2007;77:626–631.
**32** McKay WF, Peckham SM, Badura JM. A comprehensive clinical review of recombinant human bone morphogenetic protein-2 (INFUSE Bone Graft). Int Orthop 2007;31: 729–734.
**33** Barradas AM, Yuan H, van Blitterswijk CA et al. Osteoinductive biomaterials: Current knowledge of properties, experimental models and biological mechanisms. Eur Cell Mater 2011;21:407–429.
**34** Gamie Z, Tran GT, Vyzas G et al. Stem cells combined with bone graft substitutes in skeletal tissue engineering. Expert Opin Biol Ther 2012;12:713–729.
**35** Hench LL, Polak JM. Third-generation biomedical materials. Science 2002;295: 1014–1017.
**36** Rochet N, Loubat A, Laugier JP et al. Modification of gene expression induced in human osteogenic and osteosarcoma cells by culture on a biphasic calcium phosphate bone substitute. Bone 2003;32:602–610.
**37** Rodriguez R, Rubio R, Gutierrez-Aranda I et al. FUS-CHOP fusion protein expression coupled to p53 deficiency induces liposarcoma in mouse but not in human adipose-derived mesenchymal stem/stromal cells. Stem Cells 2011;29:179–192.
**38** Raval P, Hsu HH, Anderson HC. Osteoinductive ability of confluent Saos-2 cell correlates with enhanced expression of bone morphogenetic proteins. J Orthop Res 1996; 14:605–610.
**39** Trojani M, Contesso G, Coindre JM et al. Soft-tissue sarcomas of adults; study of pathological prognostic variables and definition of a histopathological grading system. Int J Cancer 1984;33:37–42.
**40** Rodriguez R, Gagou ME, Meuth M. Apoptosis induced by replication inhibitors in Chk1-depleted cells is dependent upon the helicase cofactor Cdc45. Cell Death Differ 2008;15:889–898.
**41** Abarrategi A, Moreno-Vicente C, Martinez-Vazquez FJ et al. Biological properties of solid free form designed ceramic scaffolds with BMP-2: In vitro and in vivo evaluation. Plos One 2012;7:e34117.
**42** Hao J, Ho JN, Lewis JA et al. In vivo structure–activity relationship study of dorsomorphin analogues identifies selective VEGF and BMP inhibitors. ACS Chem Biol 2010;5: 245–253.
**43** Lavery K, Swain P, Falb D et al. BMP-2/4 and BMP-6/7 differentially utilize cell surface receptors to induce osteoblastic differentiation of human bone marrow-derived mesenchymal stem cells. J Biol Chem 2008;283: 20948–20958.
**44** Rawadi G, Vayssiere B, Dunn F et al. BMP-2 controls alkaline phosphatase expression and osteoblast mineralization by a Wnt autocrine loop. J Bone Miner Res 2003;18: 1842–1853.
**45** Visvader JE. Cells of origin in cancer. Nature 2011;469:314–322.
**46** Menendez P, Catalina P, Rodriguez R et al. Bone marrow mesenchymal stem cells from infants with MLL-AF4+ acute leukemia harbor and express the MLL-AF4 fusion gene. J Exp Med 2009;206:3131–3141.
**47** Pollett JB, Corsi KA, Weiss KR et al. Malignant transformation of multipotent muscle-derived cells by concurrent differentiation signals. Stem Cells 2007;25:2302–2311.
**48** Vermeulen L, de Sousa e Melo F, Richel DJ et al. The developing cancer stem-cell model: Clinical challenges and opportunities. Lancet Oncol 2012;13:e83–89.
**49** Brune JC, Tormin A, Johansson MC et al. Mesenchymal stromal cells from primary osteosarcoma are non-malignant and strikingly similar to their bone marrow counterparts. Int J Cancer 2011;129:319–330.
**50** Shimizu T, Ishikawa T, Sugihara E et al. c-MYC overexpression with loss of Ink4a/Arf transforms bone marrow stromal cells into osteosarcoma accompanied by loss of adipogenesis. Oncogene 2010;29:5687–5699.
**51** Cleton-Jansen AM, Anninga JK, Briaire-de Bruijn IH et al. Profiling of high-grade central osteosarcoma and its putative progenitor cells identifies tumourigenic pathways. Br J Cancer 2009;101:2064.
**52** Mohseny AB, Machado I, Cai Y et al. Functional characterization of osteosarcoma cell lines provides representative models to study the human disease. Lab Invest 2011; 91:1195–1205.
**53** Sulzbacher I, Birner P, Trieb K et al. The expression of bone morphogenetic proteins in osteosarcoma and its relevance as a prognostic parameter. J Clin Pathol 2002;55:381–385.
**54** Luo X, Chen J, Song WX et al. Osteogenic BMPs promote tumor growth of human osteosarcomas that harbor differentiation defects. Lab Invest 2008;88:1264–1277.
**55** Wang L, Park P, Zhang H et al. BMP-2 inhibits the tumorigenicity of cancer stem cells in human osteosarcoma OS99-1 cell line. Cancer Biol Ther 2011;11:457–463.
**56** Zhou H, Mak W, Zheng Y et al. Osteoblasts directly control lineage commitment of mesenchymal progenitor cells through Wnt signaling. J Biol Chem 2008;283:1936–1945.
**57** Sun H, Ye F, Wang J et al. The upregulation of osteoblast marker genes in mesenchymal stem cells prove the osteoinductivity of hydroxyapatite/tricalcium phosphate biomaterial. Transplant Proc 2008;40:2645–2648.
**58** Abarrategi A, Perez-Tavarez R, Rodriguez-Milla MA et al. In vivo ectopic implantation model to assess human mesenchymal progenitor cell potential. Stem Cell Rev 2013;9:833–846.
**59** Arinzeh TL, Tran T, McAlary J et al. A comparative study of biphasic calcium phosphate ceramics for human mesenchymal stem-cell-induced bone formation. Biomaterials 2005;26:3631–3638.
**60** Rodriguez R, Tornin J, Suarez C et al. Expression of FUS-CHOP fusion protein in immortalized/transformed human mesenchymal stem cells drives mixoid liposarcoma formation. Stem Cells 2013;31: 2061–2072.

See www.StemCells.com for supporting information available online.